DOI: 10.1002/ejic.201000065

Redox Processes Involved in the Synthesis and Reactivity of Oxazolinylthiophenolato Complexes of Iron(II)/(III)

Rúbia C. R. Bottini,[a] Rogério A. Gariani,[a] César de O. Cavalcanti,[a] Franciele de Oliveira,[a] Nevilde de L. G. da Rocha,[a] Davi Back,[b] Ernesto S. Lang,[b] Peter B. Hitchcock,[c] David J. Evans,[d] Giovana G. Nunes,[a] Fábio Simonelli,[a] Eduardo L. de Sá,[a] and Jaísa F. Soares*[a]

Keywords: Iron / S ligands / Structure elucidation / Redox chemistry / Density functional calculations

The reaction of anhydrous $FeCl_2$ with 2-(4′,4′-dimethyloxazolin-2′-yl)thiophenolate (ox-phS$^-$) afforded mononuclear [Fe(ox-phS)$_2$] (**A**) and binuclear [{Fe^{III}(ox-phS)}$_2$(μ-S)$_2$] (**B**). In **B**, iron(III) and S^{2-} resulted from an unexpected redox reaction involving elemental sulfur and the iron(II) starting material. Complexes **A** and **B** co-crystallise reproducibly in a 2:1 proportion. An attempt to prepare (oxazolinylthiophenolato)-iron(III) from Li(ox-phS) and anhydrous $FeCl_3$ in the presence of *N*,*N*,*N*′,*N*′-tetramethylethane-1,2-diamine (tmen) gave another redox reaction with disulfide **D**, bis{2-(4′,4′-dimethyloxazolin-2′-yl)phenyl}disulfide (ox-phS-Sph-ox), and *trans*-[FeCl$_2$(tmen)$_2$] (**E**) as 1:1 co-crystallised products. Characterisation of all complexes included Mössbauer spectroscopy and single-crystal X-ray diffraction analysis. Quantum mechanical (TDDFT) calculations for **A** and cyclic voltammetry experiments carried out with **A** and **C** helped to distinguish between ligand- and metal-based electronic transitions and redox processes. Results add to the knowledge of the rich redox chemistry of early transition metals with soft S-donor ligands, with possible consequences for catalytic and biochemical transformations.

Introduction

Metal oxazoline and bis(oxazoline) complexes have received considerable attention in the last few years because of their use in catalytic processes, particularly asymmetric syntheses.[1] Among these (pre)catalysts, iron-containing compounds have been sought in connection with their accessible synthesis, large metal availability, reasonable catalytic performance, low cost and low toxicity.[2] Some of these complexes have also been employed in the development of fluorescent iron biosensors[3] and as small-molecule models of natural iron-scavenging siderophores.[4–6]

Reports on the preparation of iron complexes of phenylmonooxazolines and their chalcoderivatives (Scheme 1) are scarce.[7] The crystal structure of [Fe(phox)$_3$], where Hphox is the N,O-donor 2′-(2-hydroxyphenyl)oxazoline, was only published in 2002.[8] Other reports on similar complexes containing carboxylate- or isopropyl-substituted phox, or those with derived fluorophoric tripodal ligands, are even more recent.[3,4]

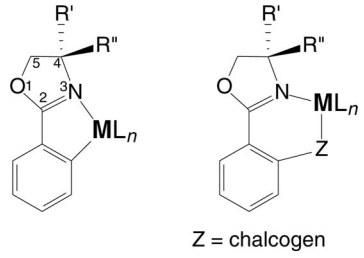

Scheme 1. Metal complexes of (chalco)phenylmonooxazolines.

To the best of our knowledge, no sulfur, selenium or tellurium analogues of Hphox have yet been shown to form stable complexes with iron, although a number of Zn^{II}, Cd^{II} and Hg^{II} adducts are known.[9,10] Considering both the relevance of iron complexes in biochemical media and the essential antioxidant activities of small molecule organochalcogens – particularly those containing sulfur and selenium – to prevent cellular damage and death,[11] literature data on the formation of iron(II)/(III) adducts of simple S- or Se-donor ligands appear to be still missing.

The present work reveals that redox processes are clearly involved in the reactivity of iron chlorides towards the monolithium salt of 2-(4′,4′-dimethyloxazolin-2′-yl)thiophenolate, Li(ox-phS). Amongst the products, two new iron ox-

[a] Departamento de Química, Universidade Federal do Paraná, 81530-900 Curitiba-PR, Brazil
Fax: +55-41-3361-3186
E-mail: jaisa@quimica.ufpr.br
[b] Departamento de Química, Universidade Federal de Santa Maria, 97105-900 Santa Maria-RS, Brazil
[c] Department of Chemistry, University of Sussex, Brighton BN1 9QJ, UK
[d] Department of Biological Chemistry, John Innes Centre, Colney, Norwich NR4 7UH, UK

Supporting information for this article is available on the WWW under http://dx.doi.org/10.1002/ejic.201000065.

azolinylthiophenolates were obtained and characterised by spectroscopic, electrochemical and diffractometric techniques. The general aim of this research was to contribute to the understanding of the redox chemistry of iron ions in the presence of relatively simple N,S-donor ligands, because of the relevance of this chemistry for a number of organometallic and bioinorganic systems.

Results and Discussion

Co-crystallised products, as well as pure new compounds, were obtained in this work. In order to make it easier to follow the discussion, Table 1 summarises basic information on the products.

Table 1. Summary of the compounds described in this work.

Product	Description	Formulation	Figure
1	Co-crystallised **A**	**A**: $[Fe^{II}(ox\text{-}phS)_2]$	1a
	and **B** (2:1)	**B**: $[\{Fe^{III}(ox\text{-}phS)\}_2(\mu\text{-}S)_2]$	1b
2	Pure **A**	$[Fe^{II}(ox\text{-}phS)_2]$	–
3	Pure **C**	$[Zn^{II}(ox\text{-}phS)_2]$	2
4	Co-crystallised **D**	**D**: $[Fe^{II}Cl_2(tmen)_2]$	3
	and **E** (1:1)	**E**: ox-phS-Sph-ox	
5	Pure **F**	"$Fe^{II}Cl_2(tmen)$"	–

Products 1–3

The new iron oxazolinylthiophenolato molecular complexes, **A** and **B**, were isolated as part of two distinct crystalline products: dark brown **1** and bright red **2** (Scheme 2).

Product **1** is reproducibly obtained upon addition of S_8 to the lithium salt of 4′,4′-dimethyl-2′-phenyloxazoline [Li(ox)]; subsequent reaction with anhydrous $FeCl_2$ is carried out in situ, without isolation of Li(ox-phS). If, alternatively, the lithium thiophenolate is filtered off, washed, dried and then allowed to react in a 2:1 proportion with $FeCl_2$, **2** is the only product.

Colourless **3** contains a zinc(II) analogue of **A**, which was prepared to help understand the spectroscopic and redox behaviour of the 2-(4′,4′-dimethyloxazolin-2′-yl)thiophenolato ligand in a coordination environment that is similar to that in **A**. The synthesis of this complex was reported earlier by Singh and co-workers,[10] although under different reaction conditions.

FTIR spectra strongly support the presence of oxazolinylthiophenolate as a ligand in all products, as medium-to-strong bands at 1603, 1592 and 1595 cm^{-1} can be assigned to ν(C=N) in **A**, **B** and **C**, respectively. Product **1** contains two bands in this region (1603 and 1592 cm^{-1}), probably due to the presence of both **A** and **B** in the crystals. All these bands are shifted to lower wavenumbers relative to the corresponding absorption of the free phenyloxazoline (1651 cm^{-1}), which provides evidence for coordination involving the heterocyclic nitrogen. C–S stretches occur at 735, 740 and 738 cm^{-1}, which is higher than in Li(ox-phS) (729 cm^{-1}), whereas the δ(C–O–C) vibrations of the five-membered rings are registered around 1052–1053 cm^{-1} in the three compounds. Bands recorded at ca. 520 cm^{-1} were tentatively assigned to metal–N stretches, whereas ν(M–S) could not be observed in the instrument detection range.

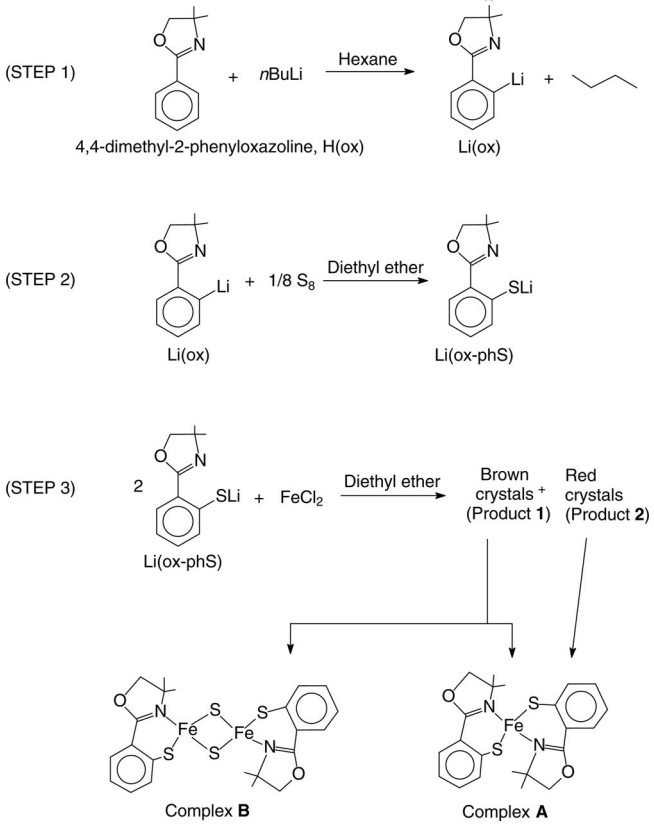

Scheme 2. Synthesis of products **1** and **2**.

Product 4

The reaction of Li(ox-phS) with anhydrous $FeCl_3$ was carried out in 1:1 and 2:1 proportions in the presence of *N*,*N*,*N*′,*N*′-tetramethylethane-1,2-diamine (tmen). In both cases, iron(III) was reduced to iron(II) and an organic disulfide was the oxidation product [Equations (1) and (2)]. The precipitation of lithium chloride from the organic medium probably contributed to the driving force of the reaction. The diamine was added to the reaction mixture to help crystallise iron-containing products, as in our earlier studies on mono-, di- and trinuclear complexes of iron(II) with tmen.[12]

$$2\,FeCl_3 + 2\,Li(ox\text{-}phS) \xrightarrow[-\,2\,LiCl]{tmen} \underset{\text{product 4 (D+E)}}{[FeCl_2(tmen)_2]\cdot(ox\text{-}phS\text{-}Sph\text{-}ox)} + \underset{\text{complex F}}{\text{"}FeCl_2(tmen)\text{"}} \quad (1)$$

$$2\,FeCl_3 + 4\,Li(ox\text{-}phS) \xrightarrow[-\,4\,LiCl]{tmen} \underset{\text{product 4 (D+E)}}{[FeCl_2(tmen)_2]\cdot(ox\text{-}phS\text{-}Sph\text{-}ox)} + \underset{\text{complex A}}{[Fe(ox\text{-}phS)_2]} \quad (2)$$

The 1:1 reaction [Equation (1)] generated bis{2-(4′,4′-dimethyl oxazolin-2′-yl)phenyl}disulfide (ox-phS-Sph-ox), which co-crystallised with *trans*-$[FeCl_2(tmen)_2]$ (**4**) as well

as "$FeCl_2$(tmen)" (**5**).[12] Product **4** was isolated from the reaction mixture as very pale yellow, well-formed rectangular prisms, whereas "$FeCl_2$(tmen)" was an off-white, microcrystalline, very air-sensitive powder.

When $FeCl_3$ and Li(ox-phS) were allowed to react in a 1:2 proportion, [Fe(ox-phS)$_2$] (**A**) was obtained together with product **4** [Equation (2)]. All three compounds (**D**, **E** and **A**) had their identities confirmed by single-crystal X-ray diffractometry and were also analysed by FTIR, Mössbauer and EPR spectroscopy. *trans*-[$FeCl_2$(tmen)$_2$] and the disulfide co-crystallise directly from the mother liquor after several days at –20 °C, whereas complex **A** crystallises independently, also at low temperature, after separation of **4** followed by careful addition of a hexane layer to the mother liquor.

The FTIR spectrum of **4** agrees with the presence of both the bis{2-(oxazolinyl)phenyl}disulfide and tmen in the light yellow crystals. In this case, the very strong, diagnostic ν(C=N) band from the oxazoline ring indicated noncoordination and was registered at almost the same wavenumber shown by the free oxazoline [1649 and 1651 cm^{-1} for the disulfide and H(ox), respectively]. This finds support in the molecular structure determined for **4** by single-crystal X-ray diffractometry. The diamine ν(C–N) vibration, in its turn, gives the relatively broad, strong band recorded at 1032 cm^{-1}, which dominates the spectrum in this region.

Synthesis and X-ray Diffraction Analyses of Products 1–3

Single-crystal X-ray diffractometry (Figures 1 and 2, with thermal ellipsoids drawn at 50% probability) and elemental analyses of products **1**–**3** confirmed their composition as listed in Table 1. Table S1 (Supporting Information) contains the crystallographic data for complex **C**.

Both **1** and **2** are air sensitive, although **1** is much less reactive. In fact, Mössbauer spectra recorded after exposure of **1** to air in the solid state for 3 d were very similar to those obtained when the sample was kept under an atmosphere of N_2 (Table S2, Supporting Information).

The crystal packing in **1** consists of layers of the dimer (perpendicular to the *c* axis) between layers of the mononuclear compound (Figure S1, Supporting Information). The tighter molecular packing in the unit cell of **1** as compared to **2** (Figures S1 and S2, Supporting Information), together with the presence of iron(III) in the binuclear compound, may explain the relative stabilities. Air sensitivity is metal based, as the zinc(II) complex (**C**) is air stable. Relevant molecular dimensions for **A** and **B** are presented in Table 2, whereas data for products **2** and **3** are shown in Table S3 (Supporting Information).

In mononuclear **A** and **C**, the metal centres are coordinated to nitrogen and sulfur donor atoms of two oxazolinylthiophenolato ligands in a distorted tetrahedral geometry. Bond lengths (Table 2) involving the metal centre in **A** are ca. 0.015–0.030 Å larger than the analogous dimensions in **C** (Table S3, Supporting Information), as expected from the difference in the ionic radii of tetracoordinate Zn^{II} and Fe^{II}

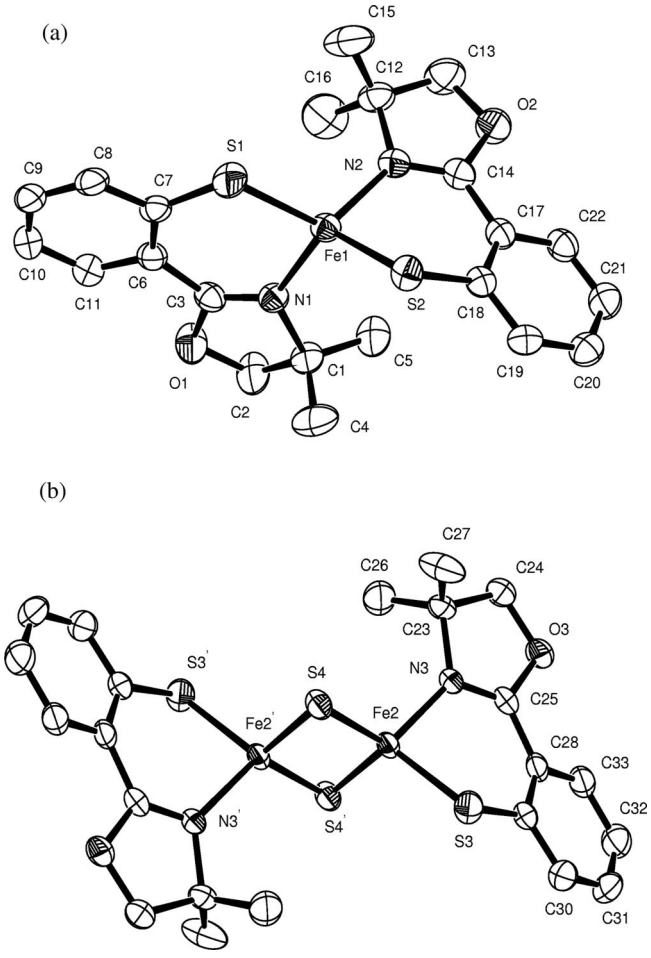

Figure 1. ORTEP-3 representations[13] of the molecular structures of (a) [Fe(ox-phS)$_2$] (complex **A**) and (b) [{Fe(ox-phS)}$_2$(μ-S)$_2$] (complex **B**).

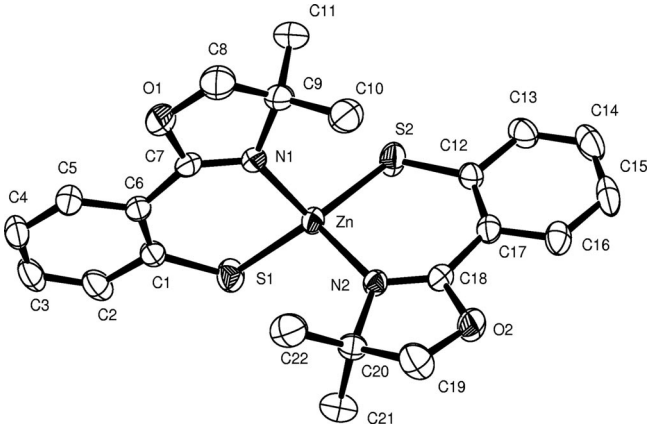

Figure 2. ORTEP-3 representation[13] of the molecular structure of [Zn(ox-phS)$_2$] (complex **C**) with the atom numbering scheme.

(0.74 and 0.77 Å respectively, the latter in high-spin state).[15] To the best of our knowledge, **A** is the first structurally characterised iron(II) complex with an N,S-phenyloxazoline ligand reported to date. In **C**, on the other hand, bond lengths and angles are very close to those reported

Table 2. Selected molecular dimensions for [Fe(ox-phS)$_2$] (**A**) and [{Fe(ox-phS)$_2$}$_2$(μ-S)$_2$] (**B**), with estimated standard deviations in parentheses.

Bond lengths about the metal centre [Å]			
A		**B**	
Fe1–N1	2.031(3)	Fe2–N3	2.022(2)
Fe1–N2	2.054(2)	Fe2–S3	2.2611(9)
Fe1–S1	2.2820(9)	Fe2–S4	2.1808(8)
Fe1–S2	2.2807(9)	Fe2–S4′	2.2014(8)
Bond angles about the metal centre [°]			
A		**B**	
N1–Fe1–N2	115.90(10)	N3–Fe2–S4′	110.07(7)
S2–Fe1–S1	113.89(3)	S4–Fe2–S3	110.75(3)
N1–Fe1–S1	95.76(8)	S4–Fe2–S4′	105.47(3)
N2–Fe1–S2	94.26(8)	N3–Fe2–S3	93.99(7)
N1–Fe1–S2	117.79(8)	S4′–Fe2–S3	117.68(4)
N2–Fe1–S1	121.02(8)	N3–Fe2–S4	119.33(7)

previously for the *Pbca* enantiomorph and different from the $P2_1$ modification.[10]

In the binuclear iron(III) product (**B**), the molecule lies on a crystallographic inversion centre located at the midpoint of the internuclear Fe2···Fe2′ axis (Figure 1b; Figure S1, Supporting Information). The structure consists of two four-coordinate iron centres, each one bound to an oxazolinylthiophenolato ligand and two bridging sulfides. The geometry about the metal centre is also distorted tetrahedral, although less distorted than in **A**. The main feature of this structure is the planar $\{Fe_2S_2\}^{2+}$ core, with unsymmetrical Fe2–S4 and Fe2–S4′ distances of 2.1808(8) and 2.2014(8) Å, respectively, which are close to the analogous dimensions in [{Fe(SCH$_2$)$_2$C$_6$H$_4$}$_2$(μ-S)$_2$]$^{2-}$ [2.185(2) and 2.232(1) Å] and in [{Fe(SC$_6$H$_4$CH$_3$)$_2$}$_2$(μ-S)$_2$]$^{2-}$ [2.200(1) and 2.202(1) Å].[16] The M–S$_{thiolate}$ and M–N bond lengths in **B** [2.2611(9) and 2.022(2) Å, respectively] are very similar to the corresponding distances in **C** and also consistent with those observed for **A** (Table 2), in spite of the different oxidation states of the iron. The M–S$_{sulfide}$ bond [av. 2.1911(8) Å] is shorter than the M–S$_{thiolate}$ analogue [2.2611(9) Å], suggesting a significant degree of π donation from the electron-rich S^{2-} ligands to the iron(III) centres. This could contribute to a softer character of the iron centres in **B** and explain why the metal in the formal oxidation states +III and +II give so similar bond lengths in **B** and **A**, respectively (Table 2).

The Fe2···Fe2′ distance in **B** is 2.6535 Å, which is one of the shortest of this type in $\{Fe_2S_2\}^{2+}$ moieties (Table 3) and consistent with a stabilising M–M interaction. This gives further support to EPR and Mössbauer spectroscopy results, discussed below. The large S4···S4′ distance (3.4875 Å), on the other hand, rules out the possibility of an S_2^{2-} anion or of any significant bonding between the two sulfur atoms. The remaining distances and angles in the central, planar 2Fe–2S ring are very much similar to those reported earlier for [Fe$_2$S$_2$(LL)$_2$]$^{2-}$ or [Fe$_2$S$_2$(L)$_4$]$^{2-}$ systems, where LL and L are bidentate(2–) and monodentate(1–) ligands, respectively (Table 3), confirming previous studies where the $\{Fe_2S_2\}$ core was found nearly invariant to the nature of the terminal ligands.[17–19]

It is known from the literature that the reaction of $FeCl_3$ with dithiols, hydrogen sulfide and sodium methoxide in methanol affords the dimeric Fe^{III} dianion [{Fe(dithiolate)}$_2$(μ-S)$_2$]$^{2-}$.[16] Complex **B** is a molecular analogue of this anion, and its formation from $FeCl_2$ probably follows iron(II) oxidation by residual S_8 [Equation (3)] in the mixture of elemental sulfur, Li(ox) and (ox-phS)$^-$. This is because the reaction of sulfur with Li(ox) was carried out in situ, and the thiolate [Li(ox-phS)] was not isolated before the addition of $FeCl_2$ [Scheme 2, Step 3; Equation (3)].

$$1/4\ S_8 + 2Fe^{II} + 2(\text{ox-phS})^- \rightarrow 2S^{2-} + 2Fe^{III} + \text{ox-phS-Sph-ox} \quad (3)$$

Also, the addition of $FeCl_2$ happened shortly after the mixture of Li(ox) and S_8, when the formation of Li(ox-phS) had probably just started. This reaction is relatively slow, and precipitation of Li(ox-phS) is only observed after ca. 1 h at room temperature. A suitable yield of the lithium thiophenyloxazolinate is only obtained after several more hours. Therefore, the conditions described in the Experimental Section were probably just right to favour the redox process that gave product **1**.

According to the literature,[20] the formation of iron–sulfur clusters containing the $\{Fe_2S_2\}^{2+}$ core from iron in low oxidation states and thiolate/disulfide mixtures is highly dependent on the nature of the thiolate and the RS$^-$/RS–SR ratio. In the present work, the presence of remaining elemental sulfur in the reaction mixture apparently determined the path of the reaction, as after its consumption the mother liquor gave only **A**. Accordingly, the combination of $FeCl_2$ with two equivalents of isolated, purified Li(ox-phS) gave a high yield of **A** without trace amounts of **B**.

Bond dimensions in the 2-(oxazolinyl)thiophenolato ligands are insensitive to the Lewis acidity of the metal ion, as clearly shown by data compiled in Table S4 (Supporting

Table 3. Selected molecular dimensions in iron–sulfur complexes containing the $\{Fe_2S_2\}^{2+}$ core. All parameters involving S atoms refer to the bridging sulfides in the central $\{Fe_2S_2\}^{2+}$ motif.[a]

Complex/Parameter	Donor set	Fe–S (av.) [Å]	S···S [Å]	Fe···Fe′ [Å]	S–Fe–S′ [°]	Fe–S–Fe′ [°]	Ref.
[{Fe(ox-phS)$_2$}$_2$(μ-S)$_2$] (**B**)	NS_3	2.1911(8)	3.4875	2.6535	105.47(3)	74.53(3)	this work
[{Fe(SCH$_2$)$_2$C$_6$H$_4$}$_2$(μ-S)$_2$]$^{2-}$	S_4	2.208(2)	3.498(3)	2.698(1)	104.74(5)	75.27(5)	[16]
[{Fe(SC$_6$H$_4$CH$_3$)$_2$}$_2$(μ-S)$_2$]$^{2-}$	S_4	2.201(1)	3.483(3)	2.691(1)	104.61(4)	75.39(4)	[16]
[{Fe(1,2-biphenolate)}$_2$(μ-S)$_2$]$^{2-}$	O_2S_2	2.215	3.512(2)	2.699(1)	104.9(1)	74.1(1)	[18]
[{Fe(pirrolate)$_2$}$_2$(μ-S)$_2$]$^{2-}$	N_2S_2	2.18	3.57(5)	2.677(1)	104.3(4)	75.7(2)	[18]
[{Fe(Fe$_2$S$_2$CO$_6$)}$_2$(μ-S)$_2$]$^{2-}$	S_4	2.198(2)	NA[a]	2.675(2)	104.96(7)	74.98(7)	[19]
[{FeCl$_2$}$_2$(μ-S)$_2$]$^{2-}$	Cl_2S_2	2.200(1)	NA[a]	2.716(1)	103.79(3)	76.21(3)	[17]

[a] NA = not available.

Information). This also compares well with structural data for metal–oxazoline complexes in higher oxidation states, such as those formed from titanium(IV) and zirconium(IV) starting materials.[21] In all these, bond lengths and angles within the oxazolinyl moiety indicate that the –C=N– bond remains localised after coordination (Table S4, Supporting Information).

The Fe1–S1 and Fe1–S2 bond lengths in **A** [2.2820(9) and 2.2807(8) Å, respectively] are very similar. The average value [2.2814(8) Å] is close to that reported for [$Fe_2(S_2$-*o*-xyl$)_3](Et_4N)_2$·2MeCN (S_2-*o*-xyl = *o*-xylene-α,α′-dithiolate; 2.2901(1) Å).[22] The average Fe–N bond length [2.0425(2) Å] is similar to that observed for [FeI_2(btmgp)], where btmgp = 1,3-bis(*N*,*N*,*N*′,*N*′-tetramethylguanidino)-propane [2.040(1) Å][23] and smaller than those reported for complexes of iron(II) with typical σ-donor ligands such as tmen,[12,24] which normally range from 2.150 to 2.280 Å.

The molecular dimensions determined for complex **A**, when obtained pure in product **2**, are very close to those found in **1** (Table 2; Table S3, Supporting Information), allowing only for slightly distinct packing pressures.

Synthesis and X-ray Diffraction Analysis of Product 4

The molecular structures of **D** and **E** (product **4**) are represented in Figure 3; relevant molecular dimensions (bond lengths and angles) are summarised in Table 4. This is the first time **D** and **E** are formed in the same reaction mixture, following oxidation of the thiophenolate by a transition-metal ion. Other reports on the synthesis of bis-[(oxazolinyl)phenyl]disulfides similar to **D** employ O_2 or aqueous $K_3[Fe(CN)_6]$ as oxidants.[10,25,26] In the present work, thiolate oxidation was accomplished under mild conditions and the use of an inert atmosphere and tmen allowed the isolation of both **D** and **E**. Their unexpected – and yet reproducible – co-crystallisation gave a significant contribution to the understanding of this [(oxazolinyl)thiophenolato]iron(III) system.

Bond dimensions in the disulfide are similar to those reported earlier for similar compounds in the pure form, suggesting that packing pressures derived from **E** are not significantly high.[10,25,26] The molecule assumes a staggered conformation (C11–S1–S2–C12 torsion angle 87.57°) to prevent repulsion between the S–S bond and lone electron pairs. The sp^3 sulfur hybridisation is evidenced by C11–S1–S2 and C12–S2–S1 angles of ca. 105° (Table 4). The S1···N1 and S2···N2 distances (av. 2.8095 Å) are much shorter than the summation of S and N van der Waals radii (3.85 Å), indicating a donor–acceptor interaction. In fact, according to the literature, the sulfur receives electron density from the nitrogen through a σ* molecular orbital of the S–S bond.[25] This helps to determine the solid-state structure of the compound. The N1···S1–S2 and N2···S2–S1 angles of 170.87 and 173.98°, respectively, indicate an almost linear N···S–S···N arrangement, compatible with a four-centre, six-electron system.[25] The molecular structure of complex **E**, in its turn, is very close to the earlier report made for *trans*-[$FeCl_2$(tmen)$_2$] by our research group.[12]

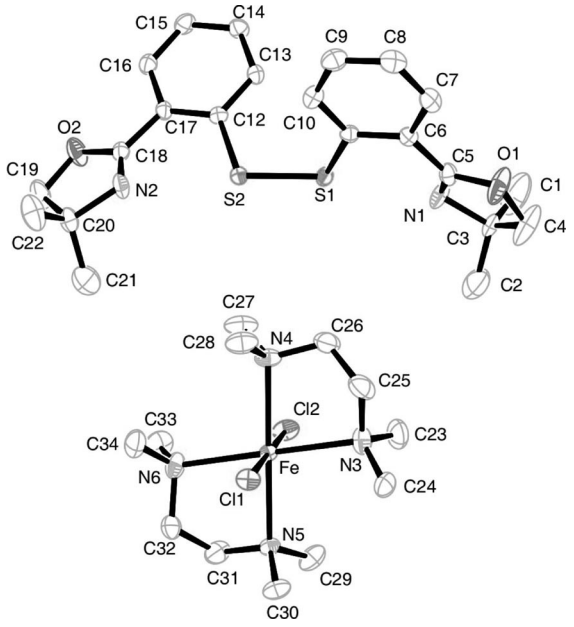

Figure 3. Representation of the molecular structures of co-crystallised *trans*-[$FeCl_2$(tmen)$_2$] and (ox-phS-Sph-ox) (product **4**) with key atoms labelled. Thermal ellipsoids are at the 50% probability level.

Table 4. Selected bond lengths [Å] and bond angles [°] for ox-phS-Sph-ox (**D**) and *trans*-[$FeCl_2$(tmen)$_2$] (**E**) with estimated standard deviations (e.s.d.s) in parentheses.

Complex **D**			
S1···N1	2.793	N2–C18	1.261(10)
S2···N2	2.826	N2–C20	1.488(9)
S1–S2	2.055(2)	C6–C11–S1	119.3(5)
S1–C11	1.793(7)	C17–C12–S2	119.1(5)
S2–C12	1.787(7)	C10–C11–S1	122.1(6)
O1–C5	1.350(9)	C13–C12–S2	121.4(5)
O2–C18	1.363(9)	C11–S1–S2	105.0(2)
N1–C5	1.257(10)	C12–S2–S1	105.4(2)
N1–C3	1.486(9)	C11–S1–S2–C12	87.57
trans-[$FeCl_2$tmen$_2$] (**E**)			
Fe–N3	2.360(7)	N3–Fe–N4	79.5(3)
Fe–N4	2.363(6)	N6–Fe–N5	80.5(2)
Fe–N5	2.371(6)	N6–Fe–N3	176.7(2)
Fe–N6	2.358(7)	N4–Fe–N5	179.4(2)
Fe–Cl1	2.4179(19)	Cl2–Fe–Cl1	178.63(8)
Fe–Cl2	2.405(2)	N3–Fe–Cl1	88.77(18)

Electron Paramagnetic Resonance (EPR) Spectroscopy

Products **1**–**4** are all EPR silent (X-band) in the solid state, both at room temperature and at 77 K. This is expected for diamagnetic zinc(II) complex **C**, and also observed for iron(II) species such as **A** and **D**, as accounted for by a large spin-orbit coupling in the ground state. The result is also compatible with a strong antiferromagnetic interaction between paramagnetic iron(III) centres in binuclear **B**, as reported for other compounds bearing the $\{Fe^{III}_2S_2\}^{2+}$ moiety.[18]

Mössbauer Spectroscopy

Two ^{57}Fe quadrupole-split doublets were recorded for the solid samples of **1**, both at room temperature and at 77 K (Figure 4 and Table 5). Doublet (a) gives Mössbauer parameters typical of high-spin iron(II), whereas doublet (b) is more difficult to attribute. A high-spin iron(III) assignment is acceptable; little temperature dependence of quadrupole splitting (q.s.) is detected (Table S2, Supporting Information). The observed values fall in the range given by other $\{Fe^{III}_2S_2\}$ complexes. An example is the $\{Fe_2S_2\}$ anion with terminal ligands derived from 2-(2-mercaptophenyl)benzimidazole, isomer shift (i.s.) = 0.25 and q.s. = 0.89 mm s^{-1}.[27] Similarly, for $\{Fe_2S_2\}$ bound to 2-hydroxybenzyl mercaptan, i.s. = 0.28, q.s. = 0.99 mm s^{-1}.[28] The large q.s. values seem characteristic of high-spin iron(III) coordinated to inflexible, tight chelate rings (as the ones generated by ox-phS), as large splittings are also found for $[Fe_2S_2L_2]^{2-}$ [L = 2,2′-biphenolate (1.02 mm s^{-1}), L = thiosalicylate (1.09 mm s^{-1}) and L = dimethyl-2,2′-methylenebis(benzimidazolate) (0.92 mm s^{-1})] in comparison to q.s. values of 0.32–0.49 mm s^{-1} for coordination by monodentate SPh, OPh, pyrrolate or the more flexible chelate S_2-o-xylyl. Therefore, a q.s. value of 1.07 mm s^{-1} for product **1** is compatible with high-spin iron(III) centres, and results from Table 5 altogether confirm the presence of a 1:1 proportion of high-spin iron(II) and iron(III) in the crystals of **1**.

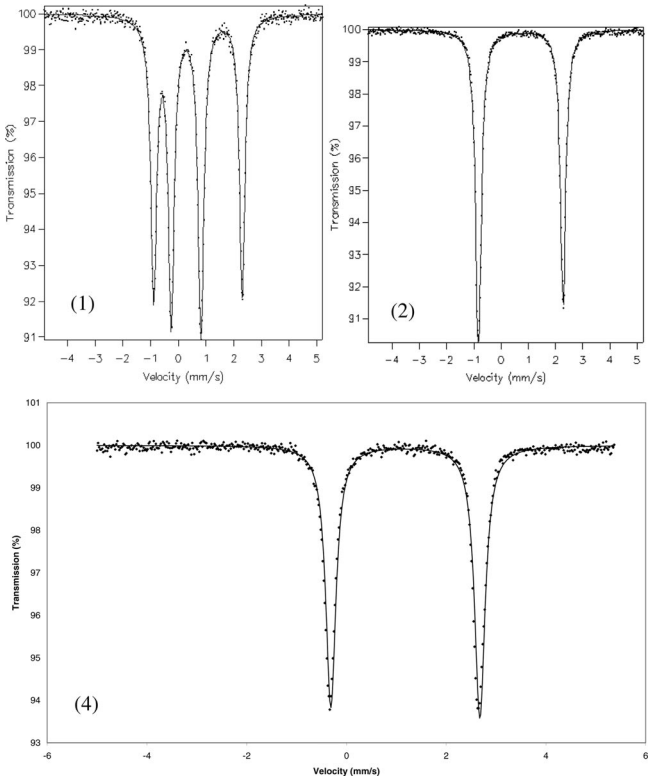

Figure 4. Zero-field ^{57}Fe Mössbauer spectra recorded at 77 K for products **1**, **2** and **4**. Reference: iron foil at 298 K.

Table 5. Zero-field ^{57}Fe Mössbauer parameters determined at 77 K for products **1**, **2** and **4**. Reference: iron foil at 298 K. Errors are <0.01 mm s^{-1}.

Parameter	Product **1**		Product **2**	Product **4**
[mm s^{-1}]	Doublet a	Doublet b		
Isomer shift	0.71	0.28	0.73	1.16
Quadrupole splitting	3.20	1.07	3.11	2.99
Γ[a]	0.13	0.13	0.13	0.13
Proportion [%]	46	54	100	100

[a] Half-width at half-height.

The isomer shifts and quadrupole splittings of the three iron(II) complexes (**1A**, **2** and **4D**) show the expected trends. The lower coordination number in the tetrahedral centres (**1A** and **2**) gives the lowest isomer shift because the s character of the hybrid orbitals on the four-coordinate iron is greater. The low symmetry around iron reduces delocalisation of the d electrons, consistent with the large quadrupole splittings in both the four- and six-coordinate environments.

Electronic Spectroscopy and Time-Dependent Density Functional Theory (TDDFT) Calculations for Complex A

Geometry optimisation and time-dependent density functional theory (TDDFT) calculations on the electronic structure of **A** employed the UB3LYP hybrid functional[29] with LANL2DZ basis set,[30] as implemented in the Gaussian03 suite.[31] The working space included 160 excited states. Tables S5 and S6 (Supporting Information) contain, respectively, the description of the frontier orbitals and electronic transitions predicted for **A**. Figure S3 (Supporting Information) presents the atom numbering scheme employed in the tables.

Frontier orbitals calculated for **A** are predominantly ligand based. Main contributions to the HOMO, HOMO-1 and HOMO-2 come from sulfur lone pairs and from benzene π orbitals. The LUMO, LUMO+2 and LUMO+3 contain a fair contribution from the iron and participate in LMCT transitions (Table S6, Supporting Information). Figure 5 shows a comparison between the experimental and calculated electronic spectra of **A**.

The experimental spectra (200–800 nm range) registered for products **1**, **2** and **3** in acetonitrile solutions are presented in Figure S4 (Supporting Information). Absorption bands are significantly strong, with molar absorptivity (ε) values ranging from 11600 to 480000 M^{-1} cm^{-1}. This is compatible with the ligand-to-ligand charge transfer (LLCT) and ligand-to-metal charge transfer (LMCT) nature of the transitions calculated by TDDFT.

In the case of **C** (product **3**; Figure S4c, Supporting Information), three intense and well-defined absorption bands were detected with ε values between 24195 and 122120 M^{-1} cm^{-1}. These were assigned to internal $p_\pi \rightarrow p_{\pi^*}$ transitions (LLCT) of the oxazolinylthiophenolato ligand. The LLCT transitions occur from molecular orbitals based

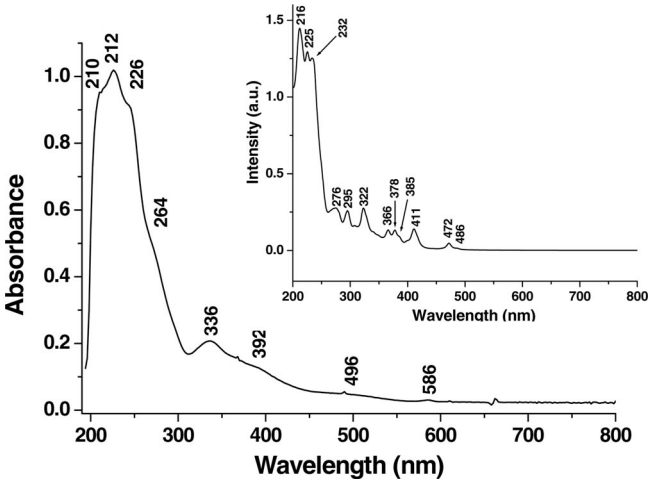

Figure 5. Experimental and calculated (TDDFT, inset) electronic spectra of [Fe(ox-phS)$_2$] (complex **A**). In the inset, only the strongest absorptions are identified. An extended list of calculated transitions is presented in Table S6 (Supporting Information).

on S and N to π* molecular orbitals of the benzene and oxazoline rings. Finally, the comparison between the electronic spectra of **A** (Figure 5; Table S6, Supporting Information) and **C** (Figure S4c, Supporting Information) confirms the general assignment of the most intense absorptions of **A**, which occur in the 200–250 nm range and around 320 nm, to LLCT transitions, whereas LMCT occurs above 250 nm. This conclusion agrees very well with data reported for the tris(chelate) [Fe(phox)$_3$].[8]

Cyclic Voltammetry

Studies on the electrochemical behaviour of H(ox) and complexes [Fe(ox-phS)$_2$] (**A**) and [Zn(ox-phS)$_2$] (**C**) were carried out at room temperature in MeCN solutions containing 0.1 M of (tba)[PF$_6$]. Voltammograms were started from 0.00 V, with scan rates of 50, 100 and 200 mV s^{-1} and a voltage window of –2.0 to +2.0 V. Representative voltammograms are presented in Figure 6. No redox processes were observed for the starting material 4,4-dimethyl-2-phenyloxazoline [H(ox)], suggesting the absence of electrochemical processes relative to the oxazoline ring in the applied potential range.

The analysis of [Zn(ox-phS)$_2$] (**C**) by cyclic voltammetry revealed two irreversible oxidation waves at +0.87 and +1.23 V (vs. Fc$^+$/Fc). These were assigned to ligand-based electrochemical processes, as no metal-centred redox reaction would be expected for zinc(II) under the employed conditions. The irreversible reduction wave observed at –1.29 V, which is not recorded in the first cycle (Figure 6a), probably corresponds to a reduction process dependent on the oxidations observed above +0.8 V. These three redox waves probably arise from the presence of sulfur as a donor atom in the ligand, as no electrochemical activity was detected for the H(ox) starting material before the incorporation of sulfur. Formation of RS$^{\cdot}$ radicals and disulfide bridges (R–S–S–R) – following thiolate oxidation – could explain the

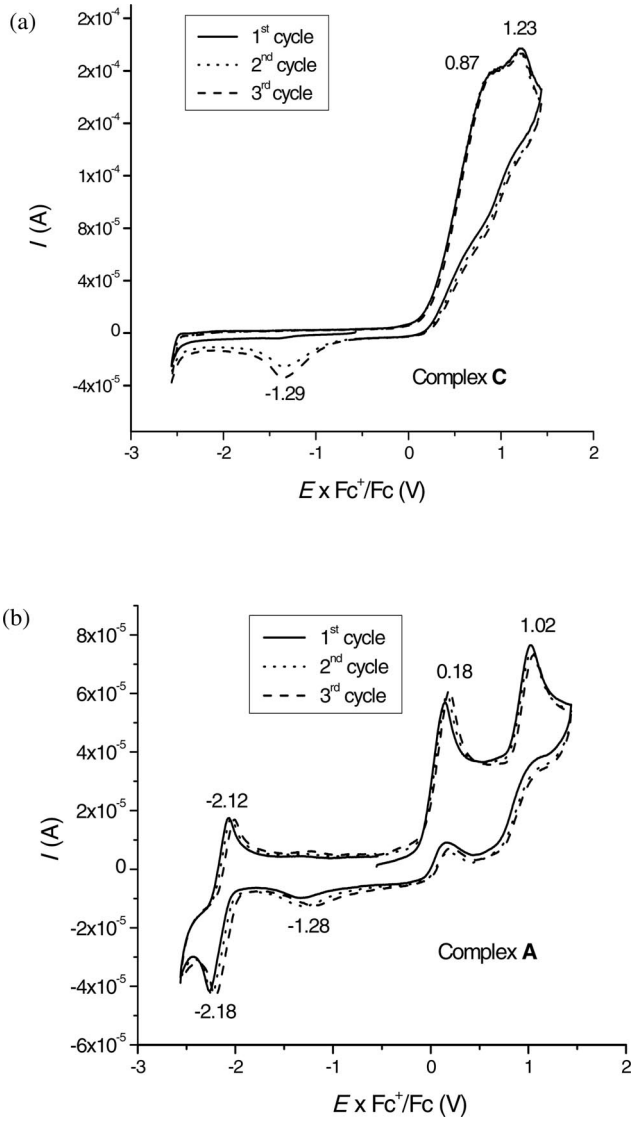

Figure 6. Cyclic voltammograms registered at 100 mV s^{-1} for (a) [Zn(ox-phS)$_2$] (**C**) and (b) [Fe(ox-phS)$_2$] (**A**) in solutions of (tba)[PF$_6$] (0.1 M) in MeCN. Potentials are referenced by $E_{1/2}$(Fc$^+$/Fc).

electroactivity of the ligand.[32] Indeed, the oxidation of (ox-phS)$^-$ to produce the respective disulfide (ox-phS-Sph-ox) has been shown to give product **4** in the present work, confirming the redox non-innocence of the sulfur-containing proligand.

For **A**, besides the oxidation waves at +0.18 and +1.02 V and the reduction at –1.28 V (which depends on the oxidations, as in **C**), a pair of waves with $E_{1/2}$ = –2.15 V is also observed. This feature does not depend on scan rates between 50 and 200 mV s^{-1}, thus indicating electrochemical reversibility, and presents a ΔE_p value half as large as that measured for the Fc$^+$/Fc pair under the same experimental conditions. The finding is compatible with a two-electron process, which was tentatively assigned to the formation of a Fe^{III} dimer, according to Equation (4) and Scheme 3. Interestingly, the process is observed even in anodic scans

from –2.50 to –2.10 V (Figure S5, Supporting Information). This suggests a high thermodynamic tendency of the system to produce the dimeric product.

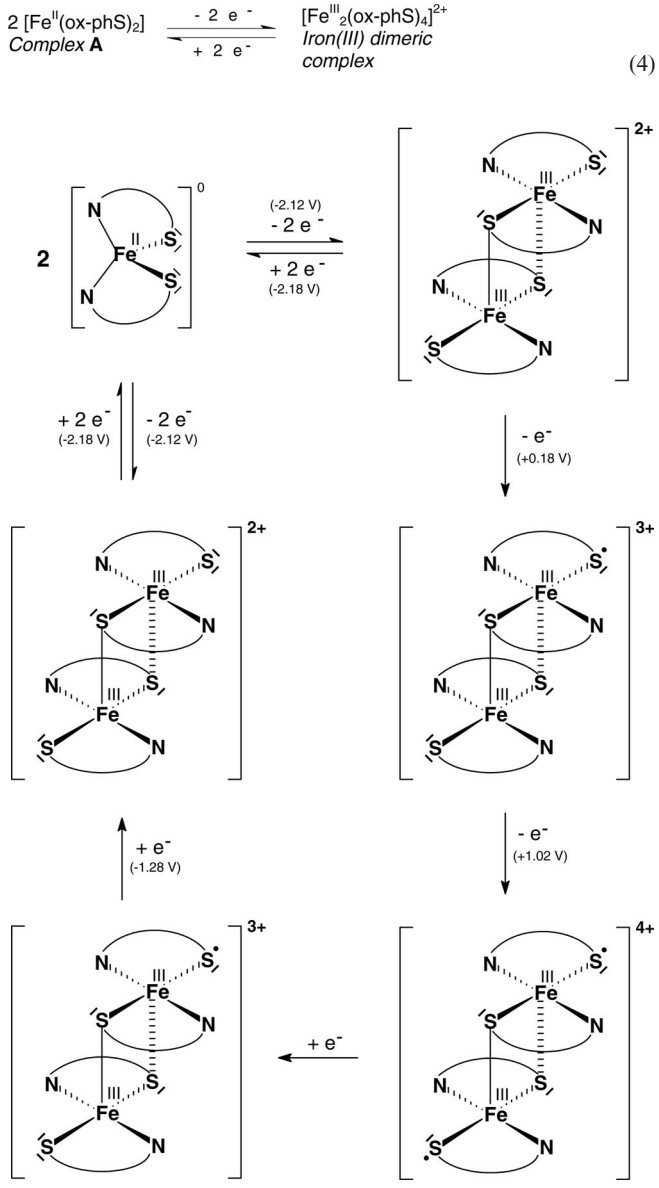

Scheme 3. Electrochemical behaviour of complex **A** under the experimental conditions employed in this work.

In the voltammogram shown in Figure S5a (Supporting Information), the reduction wave at ca. –2.20 V is not observed, indicating dependence on the oxidation at –2.10 V. Accordingly, the voltammogram in Figure S5b (Supporting Information), recorded from –2.50 to –2.10 V, shows both the oxidation and the reduction processes; this becomes clear in Figure S5c,d (Supporting Information).

Scheme 3 proposes a model for the electrochemical behaviour of complex **A**. After the formation of the dimeric Fe^{III} complex (–2.12 V), two successive oxidation processes (+0.18 and +1.02 V) could lead to the formation of $RS^{\cdot}$ radicals in the terminal ligands. The lack of electrochemical reversibility of these two processes could be explained by the formation of intermolecular bonds involving the radicals.

A number of literature reports give support to the model proposed in Scheme 3. Wieghardt and co-workers,[33] as an example, carried out a detailed electrochemical and spectroelectrochemical study on dimeric complexes of iron(III) $[N(n\text{Bu})_4][Fe_2L_4]$, where L = 1,2-benzenedithiolate, and $[N(n\text{Bu})_4][Fe_2L^{Bu}{}_4]$, where L^{Bu} = 3,5-di-*tert*-butyl-1,2-benzenedithiolate, obtained from the oxidation of the mononuclear $[N(n\text{Bu})_4][FeL_2]$ and $[N(n\text{Bu})_4][FeL^{Bu}{}_2]$, respectively, in weakly coordinating solvents. The voltammograms for the iron(III) binuclear complexes present two reversible oxidation waves, assigned to ligand-based processes, and one reversible reduction wave, which was attributed to a two-electron, metal-centred process. The latter presents $E_{1/2}$ = –1.36 V and –1.45 V (vs. Fc^+/Fc) for $[Fe_2L_4]^{2-}$ and $[Fe_2L^{Bu}{}_4]^{2-}$, respectively. According to the authors, the metal-based reduction is a two-electron transformation leading to the formation of a mononuclear iron(II) complex from the binuclear iron(III) starting compound. Equation (4) illustrates an analogous process.

A similar study describes the preparation of a dimeric Fe^{III} complex with N,S-donor ligands, $[Fe_2(\mu\text{-HNS-Ph})_2(H_2NS\text{-Ph})_2]$ (HNS-Ph = 4,6-di-*tert*-butyl-2-aminothiophenolato), from the oxidation of the related iron(II) mononuclear compound.[34] Ligand-centred processes registered for $[Fe_2L_4]^{2-}$ and $[Fe_2L^{Bu}{}_4]^{2-}$ have been assigned to the formation of $RS^{\cdot}$ radicals from the benzenedithiolate groups.[33] Indeed, the electroactivity (redox non-innocence) of S-donor ligands, such as thiolates, has been intensively investigated in other systems.[35] The comparison between the electrochemical potentials registered for the ligand-centred processes in the literature, for example, $[Fe_2L_4]^{2-}$ ($E_{1/2}$ = –0.41 and –0.10 V) and $[Fe_2L^{Bu}{}_4]^{2-}$ ($E_{1/2}$ = –0.63 and –0.35 V), with those observed in the cyclic voltammograms of **A** (E = +0.18 and +1.02 V), all vs. Fc^+/Fc, indicates that the radicals generated by L = 1,2-benzenedithiolate and L^{Bu} = 3,5-di-*tert*-butyl-1,2-benzenedithiolate are more stable than those given by oxidation of 4,4-dimethyloxazolinyl-2-thiophenolate ($ox\text{-}phS^-$) in **A**. Also, whereas the dimeric Fe^{III} products described in the literature are dianions, the dimer possibly formed from **A** is a 2+ cation, which is probably much harder to oxidise than its anionic counterparts. This agrees with Scheme 3.

Conclusions

Interestingly, in spite of the large number of reports on the preparation and catalytic performance of oxazoline complexes of a variety of transition-metal ions, the chemical literature revealed a relevant gap when referring to iron compounds with chalcogen-containing derivatives of these ligands. Results presented here, generated in a simple model system, intend to add new data to this discussion, particularly in light of the widespread biological distribution of iron(II)/(III) and of the redox-protecting in vivo activity of

sulfur- and selenium-containing biochemicals, including enzymes,[11] against reactive oxygen and nitrogen species. Iron chelation by these metabolites, or redox processes as shown here, are highly likely to change their performance, and the consequences still deserve close examination.

Experimental Section

General Procedures: All operations were carried out under an atmosphere of N_2 with the use of standard Schlenk and glove box (Vacuum Atmospheres Inc.) techniques. Solvents (Merck, J. T. Baker) were dried by standard procedures[36] and distilled under an atmosphere of N_2 prior to use. The commercial products *n*-butyllithium (1.6 M in hexane), anhydrous iron(II) and iron(III) chlorides, 2-amino-2-methylpropan-1-ol (Aldrich), potassium carbonate, ethylene glycol, glycerol and benzonitrile (Acros Organics) were used without further purification. Zinc(II) chloride (Merck) was dried by heating to ca. 300 °C under vacuum. Elemental sulfur (Reagen) was recrystallised from hot toluene. *N*,*N*,*N*′,*N*′-tetramethylethane-1,2-diamine (Amersham) was dried with KOH pellets for 24 h and then distilled under an atmosphere of N_2. 4,4-Dimethyl-2-phenyloxazoline was prepared by reaction of benzonitrile with 2-amino-2-methylpropan-1-ol in the presence of ethylene glycol, glycerol and K_2CO_3.[37] The product was extracted with hexane, dried with anhydrous Na_2SO_4 and BaO, and purified by distillation. The global yield was typically around 65%. Microanalyses were carried out by Medac Laboratories Ltd., Egham, Surrey, UK. Iron analyses were performed by a colorimetric method.[38] Zinc content was determined by differential pulse anodic stripping voltammetry (DPASV). Measurements were carried out with an EG&G Princeton Applied Research 394 Electrochemical Trace Analyser coupled with an EG&G PAR 303A static mercury drop electrode. Instrument conditions were described elsewhere.[39] IR data (Nujol mulls) were recorded with Bomem Hartmann Braun (MB series) or BIO-RAD FTS3500GX equipment in the range 400–4000 cm^{-1}. Mulls were spread on KBr plates. Zero-field ^{57}Fe Mössbauer data were recorded at 77 K and/or 300 K by using an ES-Technology MS105 spectrometer with a ^{57}Co source in a rhodium matrix. Spectra were referenced against iron foil at 298 K. Parameters were obtained by fitting the data to Lorentzian bands. EPR data (X-band, 9.5 GHz) were recorded with a Bruker ESP-300E instrument from solid samples or toluene solutions at room temperature and 77 K. Electronic spectra were obtained from toluene solutions at room temperature with a Hewlett–Packard HP 8452A diode array spectrophotometer (220–820 nm range). Magnetic susceptibility measurements by a modified Gouy method were carried out in the solid state or from toluene solutions at room temperature by using a MKII magnetic susceptibility balance from Johnson-Matthey. Corrections for the diamagnetism of the ligands were applied (Pascal constants).[40] Cyclic voltammetry experiments were controlled by using EG&G PAR 273 or Microquimica MQPG-01 potentiostats and were carried out on one-compartment glass cells with vitreous carbon (working), platinum (counter) and silver wire (pseudoreference) electrodes. The potential of the reference electrode was determined by the use of the ferrocenium/ferrocene couple (Fc^+/Fc), which occurs at +0.38 V in acetonitrile against the SCE reference electrode.[41] All redox potentials in this work are quoted vs. the $E^f(Fc^+/Fc)$. Tetra-*n*-butylammonium hexafluorophosphate, (tba)[PF_6] (Aldrich), was employed as supporting electrolyte.

Preparation of Co-Crystallised 2[Fe(ox-phS)$_2$]·[{Fe(ox-phS)}$_2$(μ-S)$_2$] (Product 1, Complexes A and B) and of Pure [Fe(ox-phS)$_2$] (Product 2, Complex A) by the In situ Preparation of Li(ox-phS) Followed by Reaction with Anhydrous $FeCl_2$: A stirred solution of 4,4-dimethyl-2-phenyloxazoline (2.5 g, 14.3 mmol) in hexane (40 mL) was treated dropwise with a solution of *n*BuLi (1.6 M in hexane, 9.1 mL, 14.3 mmol). Stirring was continued for 1 h at room temperature, giving a white precipitate, Li(ox), in an orange suspension. After decantation, the supernatant was removed by syringe, and the white solid was washed with cold hexane (15 mL), dried under vacuum (1.9 g, 10.4 mmol, 73% yield) and re-dissolved in diethyl ether (100 mL); elemental sulfur (0.33 g, 1.3 mmol S_8, 10.4 mmol "S") was added. After stirring for 1 h at room temperature, the light yellow reaction mixture was cooled down to 0 °C. A suspension of anhydrous $FeCl_2$ (0.66 g, 5.2 mmol) in toluene (35 mL) was added. Stirring was continued for 1 h at 0 °C and then for 16 h at room temperature; the brown-reddish solution was then filtered to remove lithium chloride. Dark brown crystals (0.63 g) suitable for single-crystal X-ray analysis (product **1**) were formed from this mixture after 2 d at room temperature. They were filtered off and dried under vacuum. Data for **1**: $C_{66}H_{72}Fe_4N_6O_6S_8$ (1525.18, co-crystallised complexes **A** and **B**): calcd. C 51.98, H 4.76, N 5.51, Fe 14.65; found C 51.92, H 4.76, N 5.51, Fe 14.05. IR (for **1**, **A** + **B**, Nujol mull): $\tilde{\nu}$ = 1603 (s) and 1592 [s, ν(C=N], 1366 [s, ν(C–N)], 1052 [s, δ(C–O–C)], 735 [m, ν(C–S)] cm^{-1}. UV/Vis (CH_3CN): λ (ε, $M^{-1}cm^{-1}$) = 210 (430000), 236 (480000), 274 (240000), 392 (62000), 332 (118000), 522 (35250) and 590 (29800) nm. Molar absorptivity (ε) values for **1** were based on the concentration of **A** (2.24×10^{-6} M) in the MeCN solution employed for the determination. After isolation of this first batch of **1**, the filtrate was left at room temperature for 4 d, giving a mixture of small, dark brown prisms (**1**) and bright red hexagonal crystals (product **2**). They were filtered off and dried. One day later, a pure, homogeneous batch of red crystals (**2**, 0.83 g) was isolated by filtration from the mother liquor. Total yield (**1** + **2**) based on iron content: 1.46 g, 42%. Data for **2**: $C_{22}H_{24}FeN_2O_2S_2$ (468.40): calcd. C 56.41, H 5.16, N 5.98, Fe 11.92; found C 56.39, H 5.16, N 6.09, Fe 11.43. IR (for **2**, complex **A**, Nujol mull): $\tilde{\nu}$ = 1595 [s, ν(C=N], 1369 [s, ν(C–N)], 1053 [s, δ(C–O–C)], 740 [m, ν(C–S)] cm^{-1}.

Synthesis of Pure [Fe(ox-phS)$_2$] (Product 2, Complex A) by Reaction of Anhydrous $FeCl_2$ with Isolated Li(ox-phS): The preparation of Li(ox-phS) was started as described above, from Li(ox) and elemental sulfur in diethyl ether. Soon after addition of S_8, the reaction mixture became brown-yellowish, changing to a bright yellow solution after ca. 15 min. Solid Li(ox-phS) started to precipitate after 1 h; the reaction mixture was then left to stir overnight at room temperature. The solid product (typically 50–60% yield) was isolated by filtration, dried under vacuum and stored under an atmosphere of N_2. Pure **A** was obtained from a 2:1 mixture of isolated Li(ox-phS) (0.60 g, 2.8 mmol) in diethyl ether (50 mL) and $FeCl_2$ (0.18 g, 1.4 mmol) in toluene (15 mL). After 24 h at room temperature, the dark red reaction mixture was filtered to remove LiCl; hexane (20 mL) was then carefully added as a layer. Bright red hexagonal crystals were isolated by filtration after 2 d at room temperature. Yield: 0.58 g, 88.4%. The identity of **A** was confirmed by FTIR and Mössbauer spectroscopy and by single-crystal X-ray diffraction analysis. μ_{eff} = 5.41 μ_B (room temperature). UV/Vis (CH_3CN): λ (ε, $M^{-1}cm^{-1}$) = 212 (363000), 226 (390000), 264 sh., 336 (79200), 392 (48500), 496 (18250), 586 (11600) nm.

Synthesis of [Zn(ox-phS)$_2$] (Product 3, Complex C): The procedure was analogous to that followed for pure **A** (product **2**), employing anhydrous $ZnCl_2$ (0.78 g, 5.7 mmol) and Li(ox-phS) (2.4 g, 11.4 mmol). This gave colourless crystals of [Zn(ox-phS)$_2$] (1.9 g, 68.4% yield). $C_{22}H_{24}N_2O_2S_2Zn$ (477.92): calcd. C 55.29, H 5.06, N 5.86, Zn 13.68; found C 55.48, H 5.03, N 5.87, Zn 13.47. IR (Nujol mull): $\tilde{\nu}$ = 1595 [s, ν(C=N)], 1364 [s, ν(C–N)], 1053 [s, δ(C–O–C)],

738 [s, ν(C–S)] cm^{-1}. UV/Vis (CH_3CN): λ (ε, $M^{-1}cm^{-1}$) = 250 (122120), 276 (48970), 364 (24195) nm.

Preparation of Co-Crystallised $[FeCl_2(tmen)_2]$·(ox-phS-Sph-ox) (Product 4) and "$FeCl_2$(tmen)" (Product 5) by Reaction of Anhydrous $FeCl_3$ with Isolated Li(ox-phS) and tmen (1:1:2): A very light yellow solution of Li(ox-phS) (1.5 g, 7.0 mmol) in thf (25 mL) was slowly added, at room temperature, to a stirred brown-orange suspension of $FeCl_3$ (1.1 g, 7.0 mmol) in thf (25 mL). The reaction was immediate, giving a deep brown solution that was left to stir at room temperature for 2 h. After this period, tmen (2.1 mL, 1.6 g, 13.8 mmol) was added dropwise to the reaction mixture, leading to the precipitation of a light brown solid. The suspension was filtered after 16 h of stirring at room temperature, and the solid was dried under vacuum (0.37 g, LiCl). The brown-yellowish filtrate was then evaporated under vacuum to ca. 30 mL and cooled to –20 °C for 3 weeks. This gave **4** as a colourless crystalline solid (0.66 g), which was isolated by filtration. Additional batches of these crystals were obtained after consecutive steps of evaporation of the filtrate and cooling to –20 °C. Total yield of **4**: 1.3 g, 47.5%. The identity of the product as *trans*-$[FeCl_2(tmen)_2]$·(ox-phS-Sph-ox) was confirmed by single-crystal X-ray diffraction analysis. Layering of the mother liquor with hexane also gave an off-white microcrystalline powder (**5**; 0.43 g, 50.6%), which was filtered off and dried under vacuum. The FTIR spectrum of **5** is superimposable to that of $[\{FeCl(tmen)\}_2(\mu\text{-}Cl)_2]$ prepared according to our previous report.[12] Data for **4**: $C_{34}H_{56}Cl_2FeN_6O_2S_2$ (771.72): calcd. C 52.90, H 7.33, N 10.89, Fe 7.24; found C 51.59, H 7.16, N 10.60, Fe 7.40. IR (for **4**, **D** + **E**, Nujol mull): $\tilde{\nu}$ = 1649 [vs, ν(C=N)thiophenyloxazoline], 1364 [m, ν(C–N)thiophenyloxazoline], 1076 [m, δ(C–O–C)thiophenyloxazoline], 1032 (vs), 1014 [sh., ν(C–N)diamine], 741 [m, ν(C–S)thiophenyloxazoline] cm^{-1}. IR (for **5**, Nujol mull): $\tilde{\nu}$ = 1008 [s, ν(C–N)], 1025 [vs, ν(C–N)], 442 [w, ν(Fe–N)], 463 [w, ν(Fe–N)], 486 [w, ν(Fe–N)] cm^{-1}.

Preparation of Co-Crystallised $[FeCl_2(tmen)_2]$·(ox-phS-Sph-ox) (Product 4) and $[Fe(ox\text{-}phS)_2]$ (Product 2, Complex A) by Reaction of Anhydrous $FeCl_3$ with Isolated Li(ox-phS) and tmen (1:2:2): A suspension of anhydrous $FeCl_3$ (0.75 g, 4.6 mmol) in thf (30 mL) was slowly added at room temperature to a light yellow solution of Li(ox-phS) (2.1 g, 9.7 mmol) in thf (30 mL), and the mixture was stirred for 1.5 h. To the deep red-brownish reaction mixture was added tmen (1.4 mL, 1.1 g, 9.3 mmol). No precipitation was observed. The solution was then left to stir at room temperature for 2 d, after which it was evaporated under vacuum to ca. 25 mL, layered with hexane (25 mL) and cooled to –20 °C to give red crystals of $[Fe(ox\text{-}phS)_2]$ (complex **A**, 0.56 g, 52% yield). Several subsequent steps of solvent evaporation, addition of hexane and cooling at –20 °C also gave product **4** (0.82 g, 46%).

Single-Crystal X-ray Diffraction Analyses: Details on data collections and structure refinements are presented in Table 6 and the Supporting Information. Data for **1**–**3** were collected at 173 K with a Nonius Kappa CCD area detector diffractometer at the Department of Chemistry, University of Sussex, Brighton, UK. An absorption correction (multiscan) was applied in all cases. A suitable dark brown rectangular prism of **1** ($0.15 \times 0.15 \times 0.05$ mm^3), a red hexagonal prism of **2** ($0.3 \times 0.25 \times 0.25$ mm^3) and a colourless rectangular prism of **3** ($0.25 \times 0.20 \times 0.20$ mm^3) were mounted on glass fibres and cooled to 173(2) K. Cell dimensions were based on all 5011, 3140 and 3387 observed reflections ($I > 2\sigma_I$) for **1**, **2** and **3**, respectively. Structures were solved by direct methods (WinGX)[42] and refined by full-matrix least-squares on F^2 with SHELXL-97.[14] Drawings were made with ORTEP-3 for Windows.[13] All non-hydrogen atoms were refined anisotropically, and H atoms were included in riding mode. Product **2** (complex **A**) had its crystal and molecular structures solved thrice, after being (i) co-crystallised with product **1**, (ii) obtained as the only reaction product and also (iii) prepared together with product **4**. X-ray data for

Table 6. Crystal and refinement data for $2[Fe(ox\text{-}phS)_2]$·$[\{Fe(ox\text{-}phS)\}_2(\mu\text{-}S)_2]$ (**1**), $[Fe(ox\text{-}phS)_2]$ (**2**) and $[FeCl_2(tmen)_2]$·(ox-phS-Sph-ox) (**4**).

	1 (**A** + **B**)	**2** (**A**)	**4** (**D** + **E**)
Formula	$C_{66}H_{72}N_6O_6S_8Fe_4$	$C_{22}H_{24}N_2O_2S_2Fe$	$C_{34}H_{56}Cl_2FeN_6O_2S_2$
Fw [$g\,mol^{-1}$]	1525.18	468.40	771.72
T [K]	173(2)	173(2)	293(2)
Crystal system	monoclinic	monoclinic	monoclinic
Space group	$P2_1/n$	$P2_1/n$	$P2_1/n$
a [Å]	11.0426(2)	9.3542(4)	9.0481(3)
b [Å]	10.7840(2)	11.2933(4)	16.5858(5)
c [Å]	29.4789(5)	21.4225(5)	26.0979(9)
β [°]	94.347(1)	96.666(2)	90.291(2)
V [$Å^3$]	3500.35(11)	2247.77(14)	3916.5(2)
F(000)	1580	976	1640
Z	2	4	4
$\rho_{calcd.}$ [$mg\,m^{-3}$]	1.45	1.38	1.309
μ [mm^{-1}]	1.11	0.88	0.666
θ range [°]	3.73–25.01	3.56–26.02	1.99–26.41
Measured data	28641	18125	37996
Independent data	6111	4405	7938
Data $I > 2\sigma_I$	5011	3140	7138
Parameters	406	262	424
Completeness to θ_{max} [%]	98.9	99.6	98.6
S on F^2[a]	1.055	1.016	1.157
R_1 ($I > 2\sigma_I$)[a]	0.046	0.042	0.1034
wR_2 ($I > 2\sigma_I$)[a]	0.116	0.079	0.2448
R_1 (all data)[a]	0.059	0.076	0.1093
wR_2 (all data)[a]	0.125	0.091	0.2473

[a] As defined by the SHELXL-97 program.[14]

product **4** were collected with a Bruker Kappa X8 APEX II CCD diffractometer by using Mo-K_α radiation (0.71073 Å) at the Department of Chemistry, Universidade Federal de Santa Maria, RS, Brazil. A colourless rectangular prism of **4** ($0.47 \times 0.31 \times 0.25$ mm^3) was employed for data collection at 293(2) K. X-PREP was used to perform the Gaussian absorption correction based on indexed crystal faces.[43] Cell dimensions were based on all 7938 observed reflections ($I > 2\sigma_I$, Table 6). Structure resolution (by direct methods) and refinement (by full-matrix least-squares on F^2) were carried out with SHELXS-97[44] and SHELXL-97 package[14] respectively. Refinements employed anisotropic displacement parameters for all non-hydrogen atoms, whereas H atoms were included in calculated positions. CCDC-681814 (for **1**), -681815 (for **2**), -681816 (for **3**), -725548 (for **4**) and -725547 (for **2** crystallised from the same reaction mixture that gave **4**) contain the supplementary crystallographic data for this paper. These data can be obtained free of charge from The Cambridge Crystallographic Data Centre via www.ccdc.cam.ac.uk/data_request/cif.

Supporting Information (see footnote on the first page of this article): Crystal and structure refinement data for **3**; Mössbauer parameters for **1**; selected molecular dimensions for **2** and **3**; selected bond lengths in the ligands for products **1**–**3**; frontier molecular orbitals calculated for complex **A**; electronic transitions calculated for complex **A**; crystal structure of **1** and **2**; MOLDEN representation of the molecular structure of complex **A**; electronic spectra for **1**–**3**; cyclic voltammograms for complex **A**.

Acknowledgments

We are grateful to Mr. José Luiz B. dos Santos and Mrs. Glaci Alves for help with the preparation of products **1** and **2**, to Ms. Vanessa E. dos Anjos for zinc analyses and to Dr. Geraldo R. Friedermann, Prof. Sueli Maria Drechsel and Prof. Carlos J. da Cunha (Departamento de Química, UFPR) for helpful suggestions. This work has been supported by the Conselho Nacional de Desenvolvimento Científico e Tecnológico (CNPq 309051/2006-1 and 307535/2009-6), the Coordenação de Aperfeiçoamento de Pessoal de Nível Superior (CAPES) and the Universidade Federal do Paraná (UFPR). R. C. R. B. and R. A. G. thank CAPES, and D. B., E. S. S., F. S. and J. F. S. thank CNPq for scholarships. D. J. E. thanks the Biotechnology and Biological Sciences Research Council (BBSRC) for financial support.

[1] a) C. A. Caputo, N. D. Jones, *Dalton Trans.* **2007**, 4627–4640; b) R. Rasappan, D. Laventine, O. Reiser, *Coord. Chem. Rev.* **2008**, *252*, 702–714; c) G. Desimoni, G. Faita, K. A. Jørgensen, *Chem. Rev.* **2006**, *106*, 3561–3651.

[2] a) R. Ferro, S. Milione, V. Bertolasi, C. Capacchione, A. Grassi, *Macromolecules* **2007**, *40*, 8544–8546; b) A. M. Tondreau, J. M. Darmon, B. M. Wile, S. K. Floyd, E. Lobkovsky, P. J. Chirik, *Organometallics* **2009**, *28*, 3928–3940; c) M. Zhang, R. Gao, X. Hao, W.-H. Sun, *J. Organomet. Chem.* **2008**, *693*, 3867–3877.

[3] R. Kikkeri, H. Traboulsi, N. Humbert, E. Gumienna-Kontecka, R. Arad-Yellin, G. Melman, M. Elhabiri, A.-M. Albrecht-Gary, A. Shanzer, *Inorg. Chem.* **2007**, *46*, 2485–2497.

[4] M. D. Godbole, M. P. Puig, S. Tanase, H. Kooijman, A. L. Spek, E. Bouwman, *Inorg. Chim. Acta* **2007**, *360*, 1954–1960.

[5] W. M. Wuest, E. S. Sattely, C. T. Walsh, *J. Am. Chem. Soc.* **2009**, *131*, 5056–5057.

[6] G. C. Hargaden, P. J. Guiry, *Chem. Rev.* **2009**, *109*, 2505–2550.

[7] M. Gómez, G. Muller, M. Rocamora, *Coord. Chem. Rev.* **1999**, *193–195*, 769–835.

[8] H. Kooijman, A. L. Spek, M. Hoogenraad, E. Bouwman, J. G. Haasnoot, J. Reedijk, *Acta Crystallogr., Sect. C: Cryst. Struct. Commun.* **2002**, *58*, m390–m392.

[9] a) G. Mugesh, H. B. Singh, R. J. Butcher, *J. Organomet. Chem.* **1999**, *577*, 243–248; b) G. Mugesh, H. B. Singh, R. P. Patel, R. J. Butcher, *Inorg. Chem.* **1998**, *37*, 2663–2669.

[10] G. Mugesh, H. B. Singh, R. J. Butcher, *Eur. J. Inorg. Chem.* **1999**, 1229–1236.

[11] a) E. E. Battin, J. L. Brumaghim, *Cell Biochem. Biophys.* **2009**, *55*, 1–23; b) G. Mugesh, A. Panda, H. B. Singh, N. S. Punekar, R. J. Butcher, *J. Am. Chem. Soc.* **2001**, *123*, 839–850; c) B. K. Sarma, G. Mugesh, *Org. Biomol. Chem.* **2008**, *6*, 965–974.

[12] S. C. Davies, D. L. Hughes, G. J. Leigh, J. R. Sanders, J. S. de Souza, *J. Chem. Soc., Dalton Trans.* **1997**, 1981–1988.

[13] L. J. Farrugia, *J. Appl. Crystallogr.* **1997**, *30*, 565.

[14] G. M. Sheldrich, *SHELXL-97: Program for Crystal Structure Refinement*, University of Göttingen, Germany, **1997**.

[15] J. E. Huheey, E. A. Keiter, R. L. Keiter, *Inorganic Chemistry: Principles of Structure and Reactivity*, HarperCollins, New York, **1993**, pp. 114–117.

[16] J. J. Mayerle, S. E. Denmark, B. V. DePamphilis, J. A. Ibers, R. H. Holm, *J. Am. Chem. Soc.* **1975**, *97*, 1032–1045.

[17] M. A. Bobrik, K. O. Hodgson, R. H. Holm, *Inorg. Chem.* **1977**, *16*, 1851–1858.

[18] D. Coucouvanis, A. Salifoglou, M. G. Kanatzidis, A. Simopoulos, V. Papaefthymiou, *J. Am. Chem. Soc.* **1984**, *106*, 6081–6082.

[19] F. Calderoni, F. Demartin, M. C. Iapalucci, F. Laschi, G. Longoni, P. Zanello, *Inorg. Chem.* **1996**, *35*, 898–905.

[20] G. L. Lilley, E. Sinn, B. A. Averill, *Inorg. Chem.* **1986**, *25*, 1073–1075.

[21] P. G. Cozzi, C. Floriani, A. Chiesi-Villa, C. Rizzoli, *Inorg. Chem.* **1995**, *34*, 2921–2930.

[22] K. S. Hagen, R. H. Holm, *Inorg. Chem.* **1984**, *23*, 418–427.

[23] S. Pohl, M. Harmjanz, J. Schneider, W. Saak, G. Henkel, *J. Chem. Soc., Dalton Trans.* **2000**, 3473–3479.

[24] D. J. Evans, P. B. Hitchcock, G. J. Leigh, B. K. Nicholson, A. C. Niedwieski, F. S. Nunes, J. F. Soares, *Inorg. Chim. Acta* **2001**, *319*, 147–158.

[25] A. Esparza-Ruiz, A. Peña-Hueso, J. Hernández-Díaz, A. Flores-Parra, R. Contreras, *Cryst. Growth Des.* **2007**, *7*, 2031–2040.

[26] S. Kumar, K. Kandasamy, H. B. Singh, R. J. Butcher, *New J. Chem.* **2004**, *28*, 640–645.

[27] P. Beardwood, J. F. Gibson, *J. Chem. Soc., Dalton Trans.* **1992**, 2457–2466.

[28] P. Beardwood, J. F. Gibson, *Polyhedron* **1988**, *7*, 1911–1918.

[29] a) A. D. Becke, *J. Chem. Phys.* **1993**, *98*, 5648–5652; b) C. Lee, W. Yang, R. G. Parr, *Phys. Rev. B* **1988**, *37*, 785–789; c) S. H. Vosko, L. Wilk, M. Nusair, *Can. J. Phys.* **1980**, *58*, 1200–1211; d) P. J. Stephens, F. J. Devlin, C. F. Chabalowski, M. J. Frisch, *J. Phys. Chem.* **1994**, *98*, 11623–11627.

[30] P. J. Hay, W. R. Wadt, *J. Chem. Phys.* **1985**, *82*, 270–283.

[31] M. J. Frisch, G. W. Trucks, H. B. Schlegel, G. E. Scuseria, M. A. Robb, J. R. Cheeseman, J. A. Montgomery Jr., T. Vreven, K. N. Kudin, J. C. Burant, J. M. Millam, S. S. Iyengar, J. Tomasi, V. Barone, B. Mennucci, M. Cossi, G. Scalmani, N. Rega, G. A. Petersson, H. Nakatsuji, M. Hada, M. Ehara, K. Toyota, R. Fukuda, J. Hasegawa, M. Ishida, T. Nakajima, Y. Honda, O. Kitao, H. Nakai, M. Klene, X. Li, J. E. Knox, H. P. Hratchian, J. B. Cross, V. Bakken, C. Adamo, J. Jaramillo, R. Gomperts, R. E. Stratmann, O. Yazyev, A. J. Austin, R. Cammi, C. Pomelli, J. W. Ochterski, P. Y. Ayala, K. Morokuma, G. A. Voth, P. Salvador, J. J. Dannenberg, V. G. Zakrzewski, S. Dapprich, A. D. Daniels, M. C. Strain, O. Farkas, D. K. Malick, A. D. Rabuck, K. Raghavachari, J. B. Foresman, J. V. Ortiz, Q. Cui, A. G. Baboul, S. Clifford, J. Cioslowski, B. B. Stefanov, G. Liu, A. Liashenko, P. Piskorz, I. Komaromi, R. L. Martin, D. J. Fox, T. Keith, M. A. Al-Laham, C. Y. Peng, A. Nanayakkara, M. Challacombe, P. M. W. Gill, B. Johnson, W.

Chen, M. W. Wong, C. Gonzalez, J. A. Pople, *Gaussian 03*, Revision D.01, Gaussian, Inc., Wallingford, CT, **2008**.

[32] J. S. Pap, F. L. Benedito, E. Bothe, E. Bill, S. DeBeer George, T. Weyhermuller, K. Wieghardt, *Inorg. Chem.* **2007**, *46*, 4187–4196.

[33] K. Ray, E. Bill, T. Weyhermüller, K. Wieghardt, *J. Am. Chem. Soc.* **2005**, *127*, 5641–5654.

[34] P. Ghosh, A. Begum, E. Bill, T. Weyhermüller, K. Wieghardt, *Inorg. Chem.* **2003**, *42*, 3208–3215.

[35] a) B. S. Kang, L. H. Weng, D. X. Wu, Z. Guo, L. R. Huang, Z. Y. Huang, H. Q. Liu, *Inorg. Chem.* **1988**, *27*, 1128–1130; b) C. A. Grapperhaus, S. Poturovic, *Inorg. Chem.* **2004**, *43*, 3292–3298.

[36] D. D. Perrin, W. L. F. Armarego, *Purification of Laboratory Chemicals*, 3rd ed., Butterworth-Heinemann, Oxford, **1988**, pp. 66–309.

[37] a) J. A. Frump, *Chem. Rev.* **1971**, *71*, 483–505; b) M. Reuman, A. I. Meyers, *Tetrahedron* **1985**, *41*, 837–860.

[38] A. I. Vogel, J. Basset, *Vogel's Textbook of Quantitative Inorganic Analysis*, 4th ed., Longman, New York, **1980**.

[39] E. C. Prestes, V. E. dos Anjos, F. F. Sodré, M. T. Grassi, *J. Braz. Chem. Soc.* **2006**, *17*, 53–60.

[40] G. R. Friedermann, G. G. Nunes, J. F. Soares, *Quim. Nova* **2005**, *28*, 340–344.

[41] S. J. Borg, T. Behrsing, S. P. Best, M. Razavet, X. Liu, C. J. Pickett, *J. Am. Chem. Soc.* **2004**, *126*, 16988–16999.

[42] J. Farrugia, *J. Appl. Crystallogr.* **1999**, *32*, 837–838.

[43] G. M. Sheldrick, *X-PREP*, Bruker Analytical X-ray Instruments Inc., Madison, Wisconsin, USA, **2006**.

[44] G. M. Sheldrick, *SHELXS-97: Program for Crystal Structure Solution*, University of Göttingen, Germany, **1997**.

Received: January 22, 2010
Published Online: May 5, 2010

